Two-qubit decoherence mechanisms revealed via quantum process tomography

A. G. Kofman and A. N. Korotkov
Department of Electrical Engineering, University of California, Riverside, California 92521, USA
(Received 30 March 2009; published 5 October 2009)

We analyze the quantum process tomography (QPT) in the presence of decoherence, focusing on distinguishing local and nonlocal decoherence mechanisms for a two-partite system from experimental QPT data. In particular, we consider the $\sqrt{i\mathrm{SWAP}}$ gate realized with superconducting phase qubits and calculate the QPT matrix χ in the presence of several local and nonlocal decoherence processes. We determine specific patterns of these decoherence processes, which can be used for a fast identification of the main decoherence mechanisms from an experimental χ matrix.

DOI: 10.1103/PhysRevA.80.042103 PACS number(s): 03.65.Wj, 03.65.Yz, 85.25.Cp

I. INTRODUCTION

Quantum information processing is presently a focus of significant interest since it shows a promise to perform various computational and communication tasks which are difficult or impossible to perform by classical means [1]. A standard scheme of quantum information processing involves a sequence of unitary operations (gates) on single qubits or pairs of qubits. Due to coupling to environment, the quantum-processor evolution suffers from decoherence, which introduces errors into quantum information processing. Effects of decoherence on the desired quantum evolution can be characterized by a variety of methods jointly called quantum process tomography (QPT), such as the standard QPT [1–3], ancilla-assisted process tomography (AAPT) [4–7], and direct characterization of quantum dynamics [8,9]. The standard QPT is simplest of the above methods in the sense that it can be performed with initial states being product states and local measurements of the final states.

In recent years the QPT has been demonstrated experimentally in optics [7,10–16], NMR [17–19], for ions in traps [20,21], and for solid-state qubits [22–25]. One-qubit [7,11,16,22–24], two-qubit [10,12–15,19,20,25], and three-qubit [18,21] systems have been studied. Experiments on the QPT involving more than one qubit usually use the standard QPT. The QPT experiments with the superconducting phase qubits [23–25], which are of the most interest for us here, have been also based on the standard QPT. In the present paper we also use the standard QPT.

The QPT provides a very rich (complete) information on the performance of a quantum circuit. For N qubits the QPT matrix χ [1] is generally characterized by 16^N real parameters; this number reduces to 16^N-4^N parameters if we limit ourselves by trace-preserving processes. Only 4^N-1 of these parameters correspond to a unitary evolution, while the rest of them are due to decoherence. The problem of converting experimental QPT data into a characterization of decoherence processes is of significant theoretical interest [26–31]. However, there is still no good understanding of the relation between the χ matrix elements and the decoherence parameters, except for the case of one qubit. Recently, estimation of one-qubit decoherence parameters by a QPT method was discussed in Ref. [30] for a specific decoherence model. In practice, decoherence models are often not known in advance, especially for systems containing more than one qubit. An additional complication is that often two or more unknown mechanisms simultaneously cause decoherence. In the present paper, we consider an approach to identify the decoherence models from the form of the χ matrix provided by an experiment. For that, we start with physically reasonable models of decoherence and analyze corresponding patterns in the χ matrix. If these patterns are sufficiently specific, then the main decoherence mechanisms can be identified from an experimental χ matrix directly, without a complicated numerical analysis. As a particular example we consider the $\sqrt{i\mathrm{SWAP}}$ gate made of superconducting phase qubits [32–34] and calculate the χ matrix in the presence of several local and nonlocal decoherence mechanisms, which can be anticipated for this system. We show that the patterns of significant elements of the χ matrix are quite different for different decoherence mechanisms that makes their identification relatively simple, even when two or more decoherence mechanisms simultaneously affect the system.

The paper is organized as follows. In Sec. II A we review the standard QPT for a generic system (with some formulas discussed in the Appendix) and then in Sec. II B we modify this formalism to make it more convenient for the application to a bipartite system. Section III is devoted to a brief discussion of the Markovian decoherence and calculation of its contribution into the χ matrix. In Sec. IV we introduce quantitative characteristics of the decoherence nonlocality, which can be obtained from experimental QPT data. Section V is the major part of our paper, in which we analyze the two-qubit $\sqrt{i\mathrm{SWAP}}$ gate made of superconducting phase qubits. We start with the discussion in Sec. V A of an ideal $\sqrt{i\mathrm{SWAP}}$ gate, then in Sec. V B we discuss several applicable models of local and nonlocal decoherence. In Sec. V C these models are used for the calculation of the χ matrix of the trivial (identity) two-qubit gate, then in Sec. V D the χ matrix of the $\sqrt{i\mathrm{SWAP}}$ gate is calculated for the same decoherence models (it happens to have significant similarities with the identity gate case), and these results are discussed in Sec. V E. In Sec. V F we analyze effects of decoherence on the χ matrix in the case of coupled but strongly detuned qubits. Section VI is the brief conclusion.

II. QPT BASICS

A. QPT for a generic system

According to quantum mechanics, a closed system undergoes a unitary evolution determined by the system Hamiltonian. However, usually quantum systems are coupled to environment, i.e., they are open. The evolution of an open quantum system is described [1,35] by a completely positive linear map $\mathcal{L}$ (a quantum operation): if the initial density matrix of the system and environment at time $t=0$ is a product state, $\rho^0 \otimes \rho^E$, and full evolution is described by Hamiltonian H_{SE}, then at time t the reduced density matrix of the system only is

$$\rho = \mathcal{L}[\rho^0], \quad \rho_{ij} = \sum_{k,l=0}^{d-1} \mathcal{L}_{ij,kl} \rho^0_{kl}, \tag{1}$$

where d is the dimension of the Hilbert space of the system, and the superoperator $\mathcal{L}$ has elements

$$\mathcal{L}_{ij,kl} = \sum_{i',k',l'} \langle ii'|e^{-iH_{\mathrm{SE}}t/\hbar}|kk'\rangle\langle ji'|e^{-iH_{\mathrm{SE}}t/\hbar}|ll'\rangle^* \rho^E_{k'l'}, \tag{2}$$

with i,j,k,l denoting orthonormal basis states of the system and i',k',l' denoting the environment basis states.

Besides the four-index quantity $\mathcal{L}_{ij,kl}$, it is convenient to introduce [26,36] the $d^2 \times d^2$ matrix $\boldsymbol{\mathcal{L}}$ with the same components, but indexed in a different way as follows:

$$\boldsymbol{\mathcal{L}}_{\langle ij\rangle\langle kl\rangle} = \mathcal{L}_{ij,kl}, \tag{3}$$

where we use the notation

$$\langle ij\rangle = di + j, \tag{4}$$

so that $\langle ij\rangle = 0,1,\ldots,d^2-1$ (notice mnemonic rule that the d-nary representation of the number $\langle ij\rangle$ is "ij"). Now Eq. (1) can be recast as

$$\boldsymbol{\rho} = \boldsymbol{\mathcal{L}}\boldsymbol{\rho}^0, \tag{5}$$

in which $\boldsymbol{\rho}$ is a column vector obtained by placing the rows of ρ one after another and then transposing the result, $\boldsymbol{\rho}_{\langle ij\rangle} = \rho_{ij}$.

The standard QPT [1,3] is based on a different but equivalent description of a quantum operation

$$\rho = \mathcal{L}[\rho^0] = \sum_{m,n=0}^{d^2-1} \chi_{mn} E_m \rho^0 E_n^\dagger, \tag{6}$$

where E_n are linearly independent operators (in d-dimensional Hilbert space) and χ is a $d^2 \times d^2$ Hermitian positive-semidefinite matrix, which fully characterizes the quantum operation. A quantum operation should not increase the trace of the density matrix that leads to the condition [1,12]

$$\sum_{m,n=0}^{d^2-1} \chi_{mn} E_n^\dagger E_m \le I, \tag{7}$$

where I is the (d-dimensional) identity operator. (For operators the inequality $A \le B$ means that $B-A$ is a positive operator.) For trace-preserving operations, Eq. (7) becomes an equality, while trace-decreasing operations correspond to situations when the system leaves its Hilbert space or we consider a measurement with a particular result.

The QPT matrix χ can be obtained from experimental data in two steps: first by calculating the matrix $\boldsymbol{\mathcal{L}}$ and then converting it into the χ matrix. To obtain $\boldsymbol{\mathcal{L}}$ one needs to prepare d^2 linearly independent initial states ρ_n^0 (chosen out of experimental convenience), perform the evolution, and measure the resulting states ρ_n using the quantum state tomography [1,37]. Using Eq. (5), we can write $R = \boldsymbol{\mathcal{L}} R_0$, where R and R_0 are $d^2 \times d^2$ matrices constructed from ρ_n and ρ_n^0 as

$$R_{\langle ij\rangle n} = (\rho_n)_{ij}, \quad (R_0)_{\langle ij\rangle n} = (\rho_n^0)_{ij}, \tag{8}$$

so that the nth column of R is $\boldsymbol{\rho}_n$, and similarly for R_0. Therefore, the matrix $\boldsymbol{\mathcal{L}}$ can be obtained [2] as

$$\boldsymbol{\mathcal{L}} = R R_0^{-1}, \tag{9}$$

where the existence of R_0^{-1} is ensured by the linear independence of the states ρ_n^0.

Calculation of the χ matrix from $\boldsymbol{\mathcal{L}}$ is the easiest when the operators E_n used in definition (6) form the "by-element" basis

$$F_{\langle ij\rangle} = |i\rangle\langle j|, \tag{10}$$

which we will call the "elementary basis" F_n. This is because Eq. (1) can be rewritten in a form similar to Eq. (6) as

$$\rho = \sum_{m,n=0}^{d^2-1} J_{mn} F_m \rho^0 F_n^\dagger, \tag{11}$$

where $d^2 \times d^2$ matrix J contains the same elements as $\boldsymbol{\mathcal{L}}$, but in a different order,

$$J_{\langle ij\rangle\langle kl\rangle} = \boldsymbol{\mathcal{L}}_{\langle ik\rangle\langle jl\rangle}. \tag{12}$$

Therefore, for the elementary basis, $E_n = F_n$, we obtain $\chi = J$, so that the χ matrix consists of reordered elements of $\boldsymbol{\mathcal{L}}$. Explicitly, this reordering is the following: (1) each row of $\boldsymbol{\mathcal{L}}$ is converted into a $d \times d$ matrix by sequentially placing the strings of d elements below each other and (2) these matrices are placed from left to right, with a new row of matrices starting after each d steps. (Another reordering of the matrix elements of $\boldsymbol{\mathcal{L}}$ is also often used in the literature [4,38–42]: the operator C, which is related to J as $J_{\langle ij\rangle\langle kl\rangle} = C_{\langle ji\rangle\langle lk\rangle}$ [43]. Operators C and J are called Choi or Jamiolkowski operators. Both C and J are Hermitian and positive definite.)

To obtain χ matrix for a general operator basis E_n, let us construct the $d^2 \times d^2$ matrix $\boldsymbol{E}$, whose nth column contains all elements of the $d \times d$ matrix E_n, so that $\boldsymbol{E}_{\langle ij\rangle n} = (E_n)_{ij}$. Then, $E_n = \sum_{m=0}^{d^2-1} F_m \boldsymbol{E}_{mn}$ and hence $F_n = \sum_{m=0}^{d^2-1} E_m (\boldsymbol{E}^{-1})_{mn}$, where $\boldsymbol{E}^{-1}$ exists because of the linear independence of E_n. In this way from Eq. (11) we obtain

$$\chi = \boldsymbol{E}^{-1} J (\boldsymbol{E}^{-1})^\dagger. \tag{13}$$

This expression simplifies in an important special case of mutually orthogonal operators E_n, which satisfy equation

$$\mathrm{Tr}(E_n^\dagger E_m) = d\delta_{nm}, \tag{14}$$

where δ_{nm} is the Kronecker symbol and the convenient normalization factor d allows us to include the unity operator into the set E_n (as well as products of Pauli matrices for multiqubit systems). Generalization to a different normalization is trivial—see below. In this special case $(\boldsymbol{E}^\dagger\boldsymbol{E})_{nm} = \sum_{i,j=0}^{d-1} \boldsymbol{E}^*_{\langle ij\rangle n}\boldsymbol{E}_{\langle ij\rangle m} = \mathrm{Tr}(E_n^\dagger E_m) = d\delta_{nm}$, i.e., $\boldsymbol{E}^\dagger\boldsymbol{E} = dI$ (in other words, $\boldsymbol{E}/\sqrt{d}$ is a unitary matrix), and therefore Eq. (13) becomes

$$\chi = d^{-2}\boldsymbol{E}^\dagger J\boldsymbol{E}. \tag{15}$$

In case (14) the calculation of the trace of the both sides of Eq. (7) results in the inequality

$$\mathrm{Tr}\,\chi \le 1, \tag{16}$$

which becomes the equality for a trace-preserving map.

An important example of the orthogonal unitary-operator basis E_n [satisfying Eq. (14)] for a system of N qubits is the so-called Pauli basis, which consists of tensor products of N operators from the set $\{I,X,Y,Z\}$, where X,Y,Z are the Pauli operators. The modified Pauli basis with $Y \to -iY$ is also used in the literature, for example, in the QPT analysis for one and two qubits in Refs. [1,3].

Notice that if in Eq. (14) the normalization factor d is replaced with an arbitrary number Q, then in Eq. (15) the factor d^{-2} is replaced with Q^{-2} and Eq. (16) becomes $\mathrm{Tr}\,\chi \le d/Q$. In particular, $Q=1$ for the orthonormal basis F_n introduced by Eq. (10); in this case $\boldsymbol{E}=I$, and therefore Eq. (15) reduces to the previous result $\chi=J$.

Several useful formulas for the χ matrix are discussed in the Appendix. Notice that the QPT calculation procedure discussed above is slightly different and simpler than in Refs. [1,3]; in particular, it involves an inversion of a $d^2\times d^2$ matrix [Eq. (9)] instead of a pseudoinverse calculation for a $d^4\times d^4$ matrix.

At the end of this subsection let us briefly discuss the idea of the AAPT [4–7], even though we will not use it in this paper. To perform the AAPT on a d-level system $\mathcal{S}$, one needs a similar d-level ancillary system $\mathcal{S}'$. The compound system is prepared in the maximally entangled state $|\Phi\rangle = d^{-1/2}\sum_{i=0}^{d-1}|ii\rangle$, then the quantum operation $\mathcal{L}$ is applied to the system $\mathcal{S}$ only, and then the resulting density matrix of the compound system is measured by the quantum state tomography. It is easy to see that the resulting density matrix is $(\mathcal{L}\otimes\mathcal{I})[|\Phi\rangle\langle\Phi|] = d^{-1}J$, where $\mathcal{I}$ is the identity map. In this way the matrix J is obtained directly and may later be converted into the χ matrix, as discussed above. In principle, other initial states can be also used for the AAPT, however the maximally entangled state $|\Phi\rangle$ is the optimal one [6].

B. QPT for a bipartite system

Now, let us consider a bipartite system $\mathcal{S}$ consisting of subsystems $\mathcal{S}_1$ and $\mathcal{S}_2$ with the Hilbert-space dimensions d_1 and d_2, respectively. Then the dimension of the Hilbert space of $\mathcal{S}$ is $d=d_1d_2$, and as the basis we can use the states

$$|j\rangle = |j_1\rangle|j_2\rangle \equiv |j_1j_2\rangle, \tag{17}$$

constructed out of orthonormal basis states in two subsystems. We enumerate the states using slightly generalized notation (4), so that $j=\langle j_1j_2\rangle = d_2j_1+j_2$.

As discussed in the previous subsection, the χ matrix can be calculated by performing the quantum operation on d^2 initial states ρ_n^0. It is often convenient to use the product states, $\rho^0_{\langle n_1n_2\rangle} = \rho^{(1)}_{n_1}\otimes\rho^{(2)}_{n_2}$ (where $\langle n_1n_2\rangle = d_2^2n_1+n_2$) with linearly independent sets of states for each subsystem. In this case the calculation of the matrix $\boldsymbol{\mathcal{L}}$ via Eq. (9) may be simplified; however, this requires some modification [43] of Eq. (9). The reason is that the matrix R_0 does not coincide with the Kronecker product $R_0^{(1)}\otimes R_0^{(2)}$, as may be naively expected, but requires an additional permutation of rows. As the result, it is easier to calculate first the matrix $\boldsymbol{\mathcal{L}}' = R[(R_0^{(1)})^{-1}\otimes(R_0^{(2)})^{-1}]$, and then obtain $\boldsymbol{\mathcal{L}}$ by permutation of columns, $\boldsymbol{\mathcal{L}}'_{m\langle i_1j_1i_2j_2\rangle} = \boldsymbol{\mathcal{L}}_{m\langle i_1i_2j_1j_2\rangle}$, where the four-number notation in indices is the natural generalization of notation (4): $\langle i_1j_1i_2j_2\rangle = i_1d_1d_2^2 + j_1d_2^2 + i_2d_2 + j_2$ and $\langle i_1i_2j_1j_2\rangle = i_1d_1d_2^2 + i_2d_1d_2 + j_1d_2 + j_2$.

In particular, for a two-qubit system with the initial states chosen as products of the states [1–3] $\rho_n^{(1)}=\rho_n^{(2)}=|\psi_n\rangle\langle\psi_n|$ with $|\psi_0\rangle=|0\rangle$, $|\psi_1\rangle=|1\rangle$, $|\psi_2\rangle=(|0\rangle+|1\rangle)/\sqrt{2}$, and $|\psi_3\rangle=(|0\rangle+i|1\rangle)/\sqrt{2}$, we obtain

$$(R_0^{(1)})^{-1} = (R_0^{(2)})^{-1} = \begin{pmatrix} 1 & -(1+i)/2 & (-1+i)/2 & 0 \\ 0 & -(1+i)/2 & (-1+i)/2 & 1 \\ 0 & 1 & 1 & 0 \\ 0 & i & -i & 0 \end{pmatrix}. \tag{18}$$

As discussed in the previous subsection, the calculation of the χ matrix is the easiest when for the operator basis E_n we choose the elementary basis (10). Then, $\chi=J$, where J is given by Eq. (12). However, for a bipartite system it is convenient to use the product of operator bases for each subsystem,

$$E_{\langle n_1n_2\rangle} = E^{(1)}_{n_1}\otimes E^{(2)}_{n_2}, \tag{19}$$

and the product of the elementary bases for each subsystem is not the elementary basis (10) because of the different enumeration. Therefore, to simplify formulas for a bipartite system, we have to somewhat modify the formulas for the generic system. In particular, for the product $F^{(1)}_{n_1}\otimes F^{(2)}_{n_2}$ of the elementary bases (10), we get $\chi=\tilde{J}$, where $\tilde{J}_{\langle i_1k_1i_2k_2\rangle\langle j_1l_1j_2l_2\rangle} = \boldsymbol{\mathcal{L}}_{\langle i_1i_2j_1j_2\rangle\langle k_1k_2l_1l_2\rangle}$. (The relation between $\tilde{J}$ and J is $\tilde{J}_{\langle i_1k_1i_2k_2\rangle\langle j_1l_1j_2l_2\rangle} = J_{\langle i_1i_2k_1k_2\rangle\langle j_1j_2l_1l_2\rangle}$.)

For basis (19) which uses arbitrary orthogonal subsystem bases $E_n^{(1)}$ and $E_n^{(2)}$, satisfying equations

$$\mathrm{Tr}(E_n^{(1)\dagger}E_m^{(1)}) = d_1\delta_{nm}, \quad \mathrm{Tr}(E_n^{(2)\dagger}E_m^{(2)}) = d_2\delta_{nm}, \tag{20}$$

the χ matrix can be expressed via $\tilde{J}$ as

$$\chi = d^{-2}(\boldsymbol{E}^{(1)\dagger} \otimes \boldsymbol{E}^{(2)\dagger})\tilde{J}(\boldsymbol{E}^{(1)} \otimes \boldsymbol{E}^{(2)}), \tag{21}$$

which is similar to Eq. (15) [a straightforward application of Eq. (15) would not have the desired Kronecker-product form]. Notice that if subsystem bases satisfy the orthogonality condition (20), then the compound basis (19) satisfies the orthogonality condition (14) with the normalization factor $d=d_1d_2$. Therefore, Eq. (16) remains valid, so that for a trace-preserving operation Tr $\chi=1$. In particular, for a two-qubit system and the Pauli basis we have

$$d=4, \quad \boldsymbol{E}^{(1)}=\boldsymbol{E}^{(2)}=\begin{pmatrix} 1 & 0 & 0 & 1 \\ 0 & 1 & -i & 0 \\ 0 & 1 & i & 0 \\ 1 & 0 & 0 & -1 \end{pmatrix}. \tag{22}$$

III. MARKOVIAN DECOHERENCE

A. General formalism

An important special case of a general quantum evolution is the Markovian evolution

$$\dot{\rho} = M[\rho], \tag{23}$$

where $(M[\rho])_{ij}=\Sigma_{k,l=0}^{d-1}M_{ij,kl}\rho_{kl}$ and the superoperator M is the generator of a quantum Markovian semigroup [35]. The four-index representation of M can be converted into a $d^2\times d^2$ matrix $\boldsymbol{M}$ with $\boldsymbol{M}_{\langle ij\rangle\langle kl\rangle}=M_{ij,kl}$ [similar to Eq. (3)], and then

$$\boldsymbol{\mathcal{L}} = e^{\boldsymbol{M}t}. \tag{24}$$

It is often convenient to separate the evolution generator $M=L_{\mathrm{coh}}+L$ into the coherent part $L_{\mathrm{coh}}\rho=-(i/\hbar)[H,\rho]$, with H being the Hamiltonian of the system, and the generator L of the incoherent evolution (decoherence). In the matrix form we have

$$\boldsymbol{M} = \boldsymbol{L}_{\mathrm{coh}} + \boldsymbol{L}, \quad (\boldsymbol{L}_{\mathrm{coh}})_{\langle ij\rangle\langle kl\rangle} = i(H_{lj}\delta_{ik} - H_{ik}\delta_{jl}). \tag{25}$$

In the present paper we are interested in effects of decoherence, and therefore we assume that the Hamiltonian H is known. Given the matrix $\boldsymbol{\mathcal{L}}$, which can be measured as discussed in Sec. II, the matrix $\boldsymbol{M}$ can in principle be extracted by solving Eq. (24) (although the extraction procedure involves some subtleties) [22,26,29]. Then $\boldsymbol{L}$ can be obtained from Eq. (25).

Following the QPT description (6), it is convenient to introduce a $d^2\times d^2$ matrix λ defined by the equation

$$L[\rho] = \sum_{m,n=0}^{d^2-1} \lambda_{mn}E_m\rho E_n^\dagger, \tag{26}$$

with the same operator basis E_n. The matrix λ is Hermitian and for a trace-preserving map has

$$\mathrm{Tr}\,\lambda = 0. \tag{27}$$

The matrix λ is a counterpart of the χ matrix and has many similar properties [43]. In particular, for a bipartite system and for a product basis E_n satisfying Eqs. (19) and (20), the matrix λ is given by an equation similar to Eq. (21),

$$\lambda = d^{-2}(\boldsymbol{E}^{(1)\dagger} \otimes \boldsymbol{E}^{(2)\dagger})\nu(\boldsymbol{E}^{(1)} \otimes \boldsymbol{E}^{(2)}), \tag{28}$$

where $\nu_{\langle i_1k_1i_2k_2\rangle\langle j_1l_1j_2l_2\rangle}=\boldsymbol{L}_{\langle i_1i_2j_1j_2\rangle\langle k_1k_2l_1l_2\rangle}$. Notice that $\lambda=\nu$ for the elementary product basis $F_{n1}^{(1)}\otimes F_{n2}^{(2)}$.

B. Weak decoherence

The decoherence should be relatively weak for a practical quantum information processing. In this case (for a sufficiently short time t) one can expand $\boldsymbol{\mathcal{L}}$ up to the first order in $\boldsymbol{L}$ and obtain in the interaction representation

$$\boldsymbol{\mathcal{L}}^{\mathrm{int}} = \boldsymbol{\mathcal{L}}^I + \int_0^t d\tau\, e^{-\boldsymbol{L}_{\mathrm{coh}}\tau}\boldsymbol{L}e^{\boldsymbol{L}_{\mathrm{coh}}\tau}, \tag{29}$$

where $\boldsymbol{\mathcal{L}}^I=I$ is the d^2-dimensional identity matrix and the interaction representation describes the evolution of $\rho^{\mathrm{int}}(t)=e^{iHt/\hbar}\rho(t)e^{-iHt/\hbar}$.

Further simplification is possible for a very short time or when the secular approximation [44] is applicable [43]. Then the time-dependent factors in the integrand in Eq. (29) can be omitted, yielding $\boldsymbol{\mathcal{L}}^{\mathrm{int}}=\boldsymbol{\mathcal{L}}^I+\boldsymbol{L}t$ and

$$\chi^{\mathrm{int}} = \chi^I + \lambda t, \tag{30}$$

where χ^I is the process matrix for the identity map (see the Appendix). Unfortunately, the secular approximation is usually applicable only when the subsystems (qubits or qudits) are uncoupled and there are no external fields, so that in the situations typical for quantum information processing (quantum gates) the simple Eq. (30) is not applicable. Notice that the conversion between the Schrödinger and the interaction representations for the χ matrix is (see the Appendix) $\chi=V\chi^{\mathrm{int}}V^\dagger$, where V is a unitary matrix with $V_{nm}=\mathrm{Tr}(E_n^\dagger e^{-iHt/\hbar}E_m)/d$ for the orthogonal basis E_n satisfying Eq. (14).

IV. CHARACTERISTICS OF NONLOCAL DECOHERENCE

QPT provides a wealth of information: there are d^4 independent real parameters in the matrix χ (or d^4-d^2 for a trace-preserving quantum operation), and the number of these parameters increases exponentially with the number of subsystems. However, the number of independent parameters for a multipartite system decreases drastically for local (independent) decoherence of the subsystems. In this section we discuss local decoherence of a bipartite system (generalization to a multipartite system [43] is rather straightforward).

A. Uncoupled subsystems

Let us start with assuming uncoupled subsystems, so that unitary evolution is local. If also decoherence is local, it is easy to show that for the product basis (19) the χ matrix is the Kronecker product of the corresponding χ matrices for the subsystems,

$$\chi^{\mathrm{unc}} = \chi^{(1)} \otimes \chi^{(2)}. \tag{31}$$

In this case the number of independent parameters is $\tilde{n}_\chi=d_1^4+d_2^4$ (or $\tilde{n}'_\chi=d_1^4+d_2^4-d_1^2-d_2^2$ in the trace-preserving case), which is much less than for a general χ matrix:

$n_\chi = d_1^4 d_2^4$ (or $n'_\chi = d_1^4 d_2^4 - d_1^2 d_2^2$). There is roughly a square-root decrease of complexity (Nth root decrease for an N-partite system). In particular, for a two-qubit system $\tilde{n}_\chi = 32$ and $\tilde{n}'_\chi = 24$ versus $n_\chi = 256$ and $n'_\chi = 240$.

In an experiment it is generally not known in advance whether decoherence is local or not. Therefore, a quite important information can be obtained by checking whether or not a given χ matrix has the product form (31) or, more generally, by quantifying the accuracy of the product-form approximation.

Let us define the reduced χ matrices for subsystems as

$$\tilde{\chi}^{(1)} = \mathrm{Tr}_2\, \chi, \quad \tilde{\chi}^{(2)} = \mathrm{Tr}_1\, \chi \tag{32}$$

(in more detail, $\tilde{\chi}^{(1)}_{m_1 n_1} = \Sigma_{m_2=0}^{d_2^2-1} \chi_{\langle m_1 m_2 \rangle \langle n_1 m_2 \rangle}$ and similarly for $\tilde{\chi}^{(2)}$) and introduce

$$\tilde{\chi} = \tilde{\chi}^{(1)} \otimes \tilde{\chi}^{(2)}. \tag{33}$$

A process matrix χ is factorizable if and only if $\chi = \tilde{\chi}$. For $\chi = \tilde{\chi}$ in a trace-preserving case when $\mathrm{Tr}\, \chi^{(1)} = \mathrm{Tr}\, \chi^{(2)} = \mathrm{Tr}\, \chi = 1$, the matrices $\chi^{(1)}$ and $\chi^{(2)}$ in Eq. (31) necessarily coincide with $\tilde{\chi}^{(1)}$ and $\tilde{\chi}^{(2)}$.

If $\chi \neq \tilde{\chi}$, we can introduce a dimensionless parameter ϵ_{NL} characterizing nonlocality of the decoherence,

$$\epsilon_{\mathrm{NL}} = \mathrm{Tr}|\chi - \tilde{\chi}| / \mathrm{Tr}|\chi - \chi_{\mathrm{ideal}}|, \tag{34}$$

where χ_{ideal} is the process matrix for the ideal coherent operation, which would occur in the absence of decoherence, and the absolute value of a matrix A is defined as $|A| = \sqrt{A^\dagger A}$, so that $\mathrm{Tr}|A|$ is the so-called "trace norm" of A. Since decoherence yields a deviation of χ from χ_{ideal}, the reasoning behind definition (34) is comparison of matrices $\chi - \chi_{\mathrm{ideal}}$ and $\tilde{\chi} - \chi_{\mathrm{ideal}}$ and characterization of their relative difference. For $\epsilon_{\mathrm{NL}} \ll 1$, factorization (33) is still a good approximation, while for $\epsilon_{\mathrm{NL}} \sim 1$ the decoherence is significantly nonlocal. Notice that definition (34) is meaningful only in the absence of Hamiltonian coupling between the subsystems.

B. Coupled subsystems

In the case of Markovian evolution, the nonlocality of decoherence can be checked even in the presence of a coupling between the subsystems. We assume that the coupling is included into the (known) Hamiltonian H and that the generator of the incoherent evolution L [and hence the matrix λ; see Eq. (26)] can be extracted from experimental data. For the case of local decoherence the generators $\boldsymbol{L}^{(1)}$ and $\boldsymbol{L}^{(2)}$ of the subsystems decoherence contribute to $\boldsymbol{L}$ as [43]

$$\boldsymbol{L}_{\langle i_1 i_2 j_1 j_2 \rangle \langle k_1 k_2 l_1 l_2 \rangle} = \boldsymbol{L}^{(1)}_{\langle i_1 j_1 \rangle \langle k_1 l_1 \rangle} \delta_{i_2 k_2} \delta_{j_2 l_2} + \boldsymbol{L}^{(2)}_{\langle i_2 j_2 \rangle \langle k_2 l_2 \rangle} \delta_{i_1 k_1} \delta_{j_1 l_1}, \tag{35}$$

and there is a simple relation

$$\lambda = \lambda^{(1)} \otimes \chi^{I(2)} + \chi^{I(1)} \otimes \lambda^{(2)}, \tag{36}$$

where $\chi^{I(1)}$ and $\chi^{I(2)}$ are the identity-map process matrices for the subsystems.

Similar to the discussion above, we can introduce reduced matrices $\tilde{\lambda}^{(1)} = \mathrm{Tr}_2\, \lambda$ and $\tilde{\lambda}^{(2)} = \mathrm{Tr}_1\, \lambda$ and their combination

$$\tilde{\lambda} = \tilde{\lambda}^{(1)} \otimes \chi^{I(2)} + \chi^{I(1)} \otimes \tilde{\lambda}^{(2)}. \tag{37}$$

Also similarly, it can be shown [43] that a given matrix λ has the local decoherence form (36) if and only if $\lambda = \tilde{\lambda}$. In such a case $\lambda^{(1,2)} = \tilde{\lambda}^{(1,2)}$, assuming trace-preserving operation with $\mathrm{Tr}\, \lambda^{(1)} = \mathrm{Tr}\, \lambda^{(2)} = \mathrm{Tr}\, \lambda = 0$. When $\lambda \neq \tilde{\lambda}$, the nonlocality of decoherence can be characterized by the dimensionless parameter

$$\epsilon'_{\mathrm{NL}} = \mathrm{Tr}|\lambda - \tilde{\lambda}| / \mathrm{Tr}|\lambda|. \tag{38}$$

Note that the nonlocality parameters ϵ'_{NL} and ϵ_{NL} are invariant under a change of the bases $E_n^{(1,2)}$, which preserves orthogonality [Eq. (20)]. Analysis [43] shows that $\epsilon'_{\mathrm{NL}} \approx \epsilon_{\mathrm{NL}}$ when decoherence is weak, the subsystems are uncoupled for coherent evolution, and either there is also no coherent evolution of the subsystems or the secular approximation holds.

V. EFFECTS OF DECOHERENCE MECHANISMS ON TWO-QUBIT $\sqrt{i\mathrm{SWAP}}$ GATE

Even for only two qubits, the number of decoherence parameters in the χ matrix is quite big: in a trace-preserving case we have $d^4 - 2d^2 + 1 = 225$ parameters. This corresponds to the number of generally possible decoherence processes. Obviously, the interpretation of experimental χ matrix data in such a case is quite difficult. However, instead of considering all general decoherence processes, it is meaningful to consider only physically reasonable mechanisms. Then by identifying specific features of these mechanisms in the χ matrix and comparing with experimental data, it is possible to find the magnitudes of various decoherence processes.

In this section we consider the $\sqrt{i\mathrm{SWAP}}$ gate made of superconducting phase qubits [33,34] and calculate the χ matrix assuming several plausible models of decoherence. We focus on identification of specific features of the χ matrix, which may serve as an evidence for a particular mechanism. In particular, we emphasize distinguishing local and nonlocal decoherence mechanisms.

A. $\sqrt{i\mathrm{SWAP}}$ gate

The qubit states $|0\rangle$ and $|1\rangle$ of a superconducting phase qubit [32] are the ground and the first excited states in the potential well. In this section (except Sec. V F) we assume that the two qubits are in exact resonance and use the rotating frame, which zeroes the Hamiltonians of the individual (uncoupled) qubits. Then the Hamiltonian of the capacitively coupled qubits in the rotating frame has the form [33,45]

$$H = (\hbar S/2)(|01\rangle\langle 10| + |10\rangle\langle 01|), \tag{39}$$

where S is the coupling strength (we assume that S is real). The Hamiltonian (39), which can be recast as $H = (\hbar S/4)(X \otimes X + Y \otimes Y)$, is a special case of the exchange Hamiltonian, the so called XY Hamiltonian. It was extensively discussed in relation to quantum computation. Estimation of the exchange Hamiltonian by means of the QPT was discussed in Refs. [30,31].

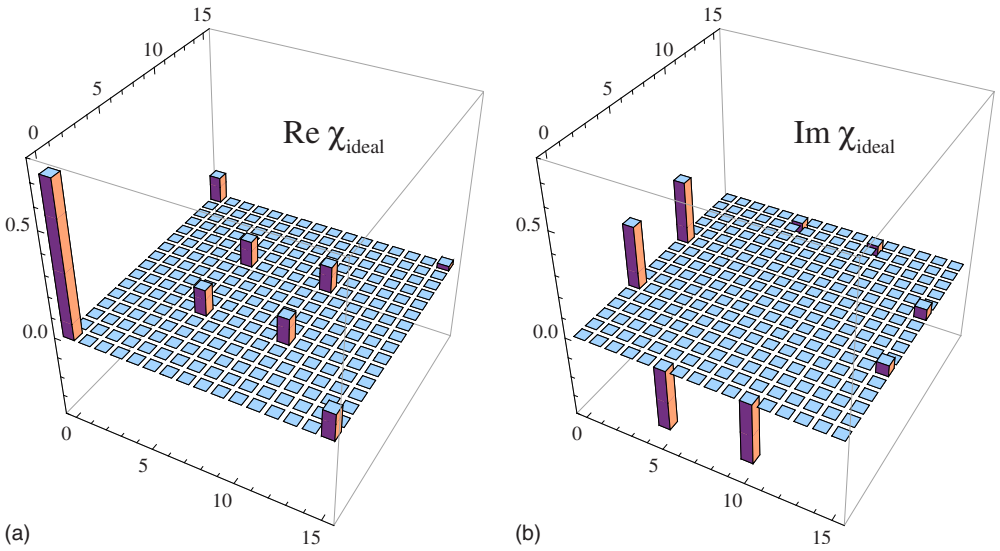

FIG. 1. (Color online) The process matrix χ_{ideal} for the perfect $\sqrt{i\text{SWAP}}$ gate in the Pauli basis. The left and right panels show, respectively, the real and imaginary parts of the (dimensionless) elements of the χ matrix. The numbering $0,1,\ldots,15$ on the two horizontal axes corresponds to $II,IX,IY,IZ,XI,XX,\ldots,ZZ$.

The evolution of the two-qubit system is then described by the unitary operator

$$U(t) = e^{-iHt/\hbar} = |00\rangle\langle 00| + |11\rangle\langle 11| + \cos(St/2)(|01\rangle\langle 01| + |10\rangle\langle 10|) - i\sin(St/2)(|01\rangle\langle 10| + |10\rangle\langle 01|). \quad (40)$$

For a noninteger value of $tS/2\pi$, gate (40) is an entangling gate and, therefore, together with one-qubit gates, it is sufficient for quantum computation [46]. In particular, $U(\pi/S)$ provides the iSWAP gate [47], while $U(\pi/2S) \equiv U_{\sqrt{i\text{SWAP}}}$ is the $\sqrt{i\text{SWAP}}$ gate [48]. For phase qubits the operation of the $\sqrt{i\text{SWAP}}$ gate has been demonstrated experimentally [33,34].

We use the Pauli basis

$$E_{\langle n_1 n_2\rangle} = X_{n_1} \otimes X_{n_2}, \quad (41)$$

where $\{X_0,X_1,X_2,X_3\}=\{I,X,Y,Z\}$, so that $\{E_0,E_1,\ldots,E_{15}\}=\{I\otimes I,I\otimes X,I\otimes Y,I\otimes Z,X\otimes I,\ldots,Z\otimes Z\}$. Note that "$n_1n_2$" is the base-4 representation of $\langle n_1 n_2\rangle$, e.g., $E_9=X_2\otimes X_1 \equiv Y\otimes X$. Operators (41) satisfy the orthogonality condition (14) with $d=4$, so that $\text{Tr}(E_n^\dagger E_m)=4\delta_{nm}$. Any linear (Kraus) operator K in the two-qubit Hilbert space can be represented as

$$K = \sum_{n=0}^{15} k_n E_n \quad (42)$$

with $k_n=\text{Tr}(E_n^\dagger K)/4$. Correspondingly, any quantum operation of the form $\rho=K\rho^0K^\dagger$ is described in the Pauli basis by the process matrix (see the Appendix)

$$\chi_{mn} = k_m k_n^*. \quad (43)$$

In the Pauli basis, Eqs. (40)–(42) (with $K=U$) yield

$$U(t) = \{[1+\cos(St/2)]I\otimes I - i\sin(St/2)(X\otimes X + Y\otimes Y) + [1-\cos(St/2)]Z\otimes Z\}/2, \quad (44)$$

and for $t=\pi/2S$ this becomes

$$U_{\sqrt{i\text{SWAP}}} = [(2+\sqrt{2})I\otimes I - i\sqrt{2}(X\otimes X + Y\otimes Y) + (2-\sqrt{2})Z\otimes Z]/4. \quad (45)$$

The process matrices χ for gates (44) and (45) can be calculated using Eq. (43). The process matrix χ_{ideal} for the perfect $\sqrt{i\text{SWAP}}$ gate is shown in Fig. 1 (since χ is Hermitian, the shown elements are symmetric about the main diagonal in the upper panel and antisymmetric in the lower panel). The nonzero elements of the matrix χ_{ideal} are

$$\chi_{00} = (3+2\sqrt{2})/8, \quad \chi_{15,15} = (3-2\sqrt{2})/8,$$

$$\chi_{55} = \chi_{10,10} = \chi_{5,10} = \chi_{10,5} = \chi_{0,15} = \chi_{15,0} = 1/8,$$

$$\chi_{05} = \chi_{0,10} = -\chi_{50} = -\chi_{10,0} = i(\sqrt{2}+1)/8,$$

$$\chi_{15,5} = \chi_{15,10} = -\chi_{5,15} = -\chi_{10,15} = i(\sqrt{2}-1)/8. \quad (46)$$

An advantage of using the Pauli basis for the χ matrix of $\sqrt{i\text{SWAP}}$ is that it results in a relatively small number of nonzero elements (eight real and eight imaginary ones) out of the total number 256. For comparison, in the elementary basis $\{|i_1i_2\rangle\langle j_1j_2|\}$ the operator $U_{\sqrt{i\text{SWAP}}}$ has six terms [see Eq. (40) with $t=\pi/2S$], resulting in $6^2=36$ nonzero terms in the χ matrix. Notice that conversion of χ_{ideal} from the Pauli basis to the modified Pauli basis (with $Y\rightarrow -iY$) would require sign change of six elements: $\chi_{10,0}$, $\chi_{10,5}$, $\chi_{10,15}$, $\chi_{0,10}$, $\chi_{5,10}$, and $\chi_{15,10}$ (in general this conversion changes 138 out of 256 elements of the χ matrix: 18 elements change sign, 60 elements are multiplied by i, and 60 elements are multiplied by $-i$).

In the presence of decoherence, the χ matrix typically acquires additional nonzero elements (in comparison with χ_{ideal}). As shown below, the positions of the most significant extra elements of χ may reveal the main mechanisms responsible for decoherence.

B. Models of decoherence

In this subsection we consider several physically reasonable decoherence models for two phase qubits (all Markovian and trace preserving), including local decoherence [49–54], correlated dephasing [55,56], and noisy coupling. In Refs. [49–56] these models have been mainly used to analyze two-qubit entanglement and Bell-inequality violation, while in this paper we focus on their effect on the χ matrix of a quantum gate. Notice that estimation of one-qubit decoherence parameters by the QPT was discussed in Ref. [30].

1. Local decoherence

First, let us consider the model of local decoherence, described by the Bloch equations [44] for each qubit, so that in the rotating frame the density matrix of a separated qubit α ($\alpha=1,2$) evolves as

$$\dot{\rho}_{11}^{(\alpha)} = -\dot{\rho}_{00}^{(\alpha)} = -\Gamma_d^{(\alpha)}\rho_{11}^{(\alpha)} + \Gamma_u^{(\alpha)}\rho_{00}^{(\alpha)},$$

$$\dot{\rho}_{10}^{(\alpha)} = -\rho_{10}^{(\alpha)}/T_2^{(\alpha)}, \tag{47}$$

where $\Gamma_d^{(\alpha)}$ and $\Gamma_u^{(\alpha)}$ are the energy-relaxation rates, so that $T_1^{(\alpha)}=(\Gamma_d^{(\alpha)}+\Gamma_u^{(\alpha)})^{-1}$ is the energy-relaxation time and $T_2^{(\alpha)}$ is the dephasing time (the Bloch equations correspond to the secular approximation for a nondegenerate two-level system weakly coupled to a bath; $\Gamma_u^{(\alpha)}=0$ for a zero-temperature bath).

Comparing Eq. (47) with the equation $\dot{\boldsymbol{\rho}}_\alpha=\boldsymbol{L}^{(\alpha)}\boldsymbol{\rho}_\alpha$, we obtain the one-qubit Markovian generators

$$\boldsymbol{L}^{(\alpha)} = \begin{pmatrix} -\Gamma_u^{(\alpha)} & 0 & 0 & \Gamma_d^{(\alpha)} \\ 0 & -1/T_2^{(\alpha)} & 0 & 0 \\ 0 & 0 & -1/T_2^{(\alpha)} & 0 \\ \Gamma_u^{(\alpha)} & 0 & 0 & -\Gamma_d^{(\alpha)} \end{pmatrix}, \tag{48}$$

while the two-qubit generator $\boldsymbol{L}_{\text{loc}}$ of the local decoherence is then given by Eq. (35), in which $\langle ijkl\rangle=8i+4j+2k+l$ (so that "$ijkl$" is the binary representation of $\langle ijkl\rangle$).

Notice that the model of local decoherence involves two decoherence mechanisms: energy relaxation and pure dephasing. Correspondingly, $\boldsymbol{L}_{\text{loc}}=\boldsymbol{L}_{\text{loc,ER}}+\boldsymbol{L}_{\text{loc,PD}}$. Technically, this splitting corresponds to representing dephasing rates as sums of two terms, $1/T_2^{(\alpha)}=(\Gamma_d^{(\alpha)}+\Gamma_u^{(\alpha)})/2+\Gamma_\alpha$, and then zeroing either Γ_α or $\Gamma_{d,u}^{(\alpha)}$.

2. Correlated dephasing

Now let us consider two models of nonlocal decoherence, starting with the model of correlated pure dephasing. For a pair of coupled phase qubits, the correlated dephasing can result from fluctuations of a common part of the magnetic field biasing qubits. We consider the system Hamiltonian $H+H_{\text{CD}}(t)$, in which H is given by Eq. (39), while the dephasing contribution is

$$H_{\text{CD}}(t) = \hbar\{\delta_1(t)|10\rangle\langle 10| + \delta_2(t)|01\rangle\langle 01| + [\delta_1(t)+\delta_2(t)]|11\rangle\langle 11|\}, \tag{49}$$

where $\delta_1(t)$ and $\delta_2(t)$ are random but partially correlated frequency shifts for the two qubits. In the derivation of Eq. (49) we neglected noise-induced transitions between the levels, assuming that the noise intensity at the qubit frequency practically vanishes.

Applying the standard method [35,57,58], we obtain the Markovian master equation for the average density matrix as follows:

$$\dot{\rho} = -(i/\hbar)[H,\rho] + L_{\text{CD}}[\rho], \tag{50}$$

$$L_{\text{CD}}[\rho] = -\begin{pmatrix} 0 & \Gamma_2\rho_{01} & \Gamma_1\rho_{02} & \Gamma_+\rho_{03} \\ \Gamma_2\rho_{10} & 0 & \Gamma_-\rho_{12} & \Gamma_1\rho_{13} \\ \Gamma_1\rho_{20} & \Gamma_-\rho_{21} & 0 & \Gamma_2\rho_{23} \\ \Gamma_+\rho_{30} & \Gamma_1\rho_{31} & \Gamma_2\rho_{32} & 0 \end{pmatrix}, \tag{51}$$

where $\Gamma_\pm=\Gamma_1+\Gamma_2\pm\bar{\Gamma}$, $\Gamma_\alpha=\int_0^\infty\langle\delta_\alpha(0)\delta_\alpha(t)\rangle dt$ ($\alpha=1,2$), $\bar{\Gamma}=\int_0^\infty\langle\delta_1(0)\delta_2(t)+\delta_2(0)\delta_1(t)\rangle dt$, and we have assumed $\langle\delta_\alpha(t)\rangle=0$. The parameter of common dephasing $\bar{\Gamma}$ is zero in the case of uncorrelated (local) dephasing, while $\bar{\Gamma}=\pm 2\sqrt{\Gamma_1\Gamma_2}$ for full correlation or anticorrelation, so that the dimensionless correlation parameter is $\kappa=\bar{\Gamma}/2\sqrt{\Gamma_1\Gamma_2}$ ($-1\le\kappa\le 1$). In the following subsections we will mainly focus on the case $\Gamma_1=\Gamma_2\equiv\Gamma_{\text{PD}}$. Notice that Eq. (51) is written in the computational basis $|j\rangle=|j_1j_2\rangle$ with $j=\langle j_1j_2\rangle=2j_1+j_2$, so that $j=0,1,2,3$ correspond to $j_1j_2=00,01,10,11$. In deriving Eqs. (50) and (51) we have assumed $\Gamma_\alpha\tau_c^{\text{CD}}\ll 1$ and $S\tau_c^{\text{CD}}\ll 1$, where τ_c^{CD} is the correlation time of the frequency fluctuations.

In discussion of the QPT it is very easy to get lost with different bases used in different equations. So we would like to repeat which bases do we use. In Eq. (51) [as well as in Eq. (53) below], we consider a two-qubit density matrix, so this 4×4 matrix uses the two-qubit basis $\{|00\rangle,|01\rangle,|10\rangle,|11\rangle\}$. Then this equation is converted into the equation for the 16×16 matrix $\boldsymbol{L}$, which uses the basis of 16 elements of the two-qubit density matrix. The matrix $\boldsymbol{\mathcal{L}}=e^{(\boldsymbol{L}_{\text{coh}}+\boldsymbol{L})t}$ uses the same by-element basis as $\boldsymbol{L}$. Finally, the matrix $\boldsymbol{\mathcal{L}}$ is converted into the 16×16 matrix χ, for which we use the basis of product-Pauli operators. Somewhat differently, in the previous subsection, Eq. (47) uses the one-qubit basis $\{|0\rangle,|1\rangle\}$ and Eq. (48) uses still one-qubit but four-dimensional by-element basis. Equation (48) is then converted into the equation for $\boldsymbol{L}$, which uses the same 16-dimensional basis as above, and further procedures coincide. Notice that the bases discussed in this paragraph have nothing to do with the set of initial states discussed in Sec. II [e.g., in the paragraph above Eq. (18)], which would be important in the experimental procedure.

3. Noisy coupling

The second nonlocal decoherence model we consider is the model of a noisy coupling. In the case of capacitively coupled phase qubits, this model corresponds to a fluctuating coupling capacitance; a more practically important case is when qubits are coupled via a tunable Josephson circuit, whose parameters may fluctuate. In the Hamiltonian (39) we substitute S with $S+s(t)$, assuming $\langle s(t)\rangle=0$. Then following the same derivation as in the previous subsection, we obtain the master equation

$$\dot{\rho}=-(i/\hbar)[H,\rho]+L_{\mathrm{NC}}[\rho], \tag{52}$$

where

$$L_{\mathrm{NC}}[\rho]=\Gamma_s\begin{pmatrix}0 & -\rho_{01} & -\rho_{02} & 0\\ -\rho_{10} & -2\rho_{11}+2\rho_{22} & -2\rho_{12}+2\rho_{21} & -\rho_{13}\\ -\rho_{20} & 2\rho_{12}-2\rho_{21} & 2\rho_{11}-2\rho_{22} & -\rho_{23}\\ 0 & -\rho_{31} & -\rho_{32} & 0\end{pmatrix} \tag{53}$$

and $\Gamma_s=(1/4)\int_0^\infty\langle s(0)s(t)\rangle dt$. In the derivation we have assumed $\Gamma_s\tau_c^{\mathrm{NC}}\ll 1$ and $S\tau_c^{\mathrm{NC}}\ll 1$, where τ_c^{NC} is the correlation time of $s(t)$.

When the discussed above decoherence mechanisms exist concurrently, the system state obviously evolves as

$$\dot{\rho}=-(i/\hbar)[H,\rho]+(L_{\mathrm{loc}}+L_{\mathrm{CD}}+L_{\mathrm{NC}})[\rho]. \tag{54}$$

By fitting experimental data with this model, it is possible to find the corresponding best-fit decoherence rates quantitatively and determine in this way if a particular decoherence mechanism is important or not. However, this is a rather laborious procedure. Another way to find out which decoherence mechanisms are important, is by checking characteristic features in the χ matrix, unique for a given mechanism. We will identify such features in the following subsections.

C. Effects of decoherence on the identity gate

Before studying the effects of decoherence on the χ matrix of the $\sqrt{i\mathrm{SWAP}}$ gate (that will be done in the next subsection), let us consider decoherence for the identity gate, i.e., for the vanishing two-qubit Hamiltonian. Then $\mathcal{L}=e^{Lt}$ with the models for the decoherence generator L discussed above, and $\mathcal{L}$ can be converted into χ in the way discussed in Sec. II B.

We are interested in effects of weak decoherence, corresponding to sufficiently short gate-operation times. In this case the process matrix for the identity gate can be approximated [see Eqs. (30) and (A8)] as

$$\chi\approx\chi^I+\lambda t,\quad \chi^I_{mn}=\delta_{m0}\delta_{n0}, \tag{55}$$

where λ is determined by Eqs. (28) and (22) (we use the Pauli basis). The matrix λ is a sum of contributions from different decoherence mechanisms, which have the following explicit forms.

For the local energy-relaxation mechanism, the nonzero matrix elements of λ in the Pauli basis are

$$\lambda_{00}=-2(\Gamma_+^{(1)}+\Gamma_+^{(2)}),$$

$$\lambda_{11}=\lambda_{22}=\Gamma_+^{(2)},\quad \lambda_{44}=\lambda_{88}=\Gamma_+^{(1)},$$

$$\lambda_{03}=\lambda_{30}=\Gamma_-^{(2)},\quad \lambda_{0,12}=\lambda_{12,0}=\Gamma_-^{(1)},$$

$$\lambda_{21}=-\lambda_{12}=i\Gamma_-^{(2)},\quad \lambda_{84}=-\lambda_{48}=i\Gamma_-^{(1)}, \tag{56}$$

where $\Gamma_\pm^{(\alpha)}=(\Gamma_d^{(\alpha)}\pm\Gamma_u^{(\alpha)})/4$ [notice a difference with the notation $\Gamma_\pm$ used in Eq. (51)]. The contribution from the local pure-dephasing mechanism is a special case of the correlated dephasing which we discuss next.

For the (correlated) pure dephasing the nonzero matrix elements of λ are

$$\lambda_{00}=-(\Gamma_1+\Gamma_2)/2,$$

$$\lambda_{33}=\Gamma_2/2,\quad \lambda_{12,12}=\Gamma_1/2,$$

$$\lambda_{3,12}=\lambda_{12,3}=-\lambda_{0,15}=-\lambda_{15,0}=\bar{\Gamma}/4. \tag{57}$$

The absence of the correlation, $\bar{\Gamma}=0$, corresponds to the local pure dephasing; in this case the third line in Eqs. (57) vanishes. For the noisy coupling the nonzero elements of λ are

$$\lambda_{00}=-\Gamma_s,\quad \lambda_{55}=\lambda_{10,10}=\lambda_{5,10}=\lambda_{10,5}=\lambda_{0,15}=\lambda_{15,0}=\Gamma_s/2. \tag{58}$$

All nonzero elements of χ except for χ_{00}, are induced by decoherence. Because of the first-order approximation (55), the most significant additional elements of χ are related approximately linearly to the nonzero elements of λ (the second-order elements of χ should be significantly smaller for a weak dephasing). Now, a very important observation is that the positions of the nonzero elements of λ (excluding λ_{00}) in Eqs. (56)–(58) are different for different decoherence models, except for $\lambda_{0,15}$ and $\lambda_{15,0}$ appearing in both Eqs. (57) and (58). Therefore, in the case of weak decoherence, *one can identify the considered decoherence mechanisms simply by the positions of the most significant (first-order) elements of* χ. Another important observation is that effects of different decoherence parameters on elements of λ are easily distinguishable. In particular, for the local decoherence model [Eqs. (56) and (57) with $\bar{\Gamma}=0$], the decoherence in the first and second qubits is completely separated, affecting different elements of λ. Similarly, for each qubit the pure dephasing is separated from energy relaxation by affecting different elements of λ, and the temperature for each qubit can be extracted from the ratio $\Gamma_-^{(\alpha)}/\Gamma_+^{(\alpha)}$, which is equal to the ratio of corresponding elements of λ in Eq. (56). The correlation factor in the pure-dephasing model can be extracted via the relative height of elements in the second and third lines of Eqs. (57) (two positive elements in the third line should be used since the negative elements are also involved in the noisy-coupling model). The clear separation of effects allows us to estimate the relative values of the decoherence parameters simply by the relative values of the corresponding elements in the χ matrix.

Such a simple analysis is possible, to a large extent, because we use the Pauli basis. The matrix λ in the Pauli basis has a relatively small number of nonzero elements. The first row in Table I shows this number for the considered deco-

TABLE I. The number of nonzero elements in the matrices λ, ν, χ, and $\tilde{J}$ for several decoherence models: energy relaxation (ER) with arbitrary or zero temperature T, local pure dephasing (LPD), local decoherence (LD) which includes both pure dephasing and energy relaxation (with $T>0$ or $T=0$), correlated pure dephasing (CD) with $0<|\kappa|<1$, completely correlated or anticorrelated pure dephasing (CCD) with $\kappa=\pm 1$, and noisy coupling (NC). We use the Pauli basis for the matrices λ and χ, while in the elementary basis they would be equal to the matrices ν and $\tilde{J}$, correspondingly. The identity gate is assumed for matrices χ and $\tilde{J}$.

	$ER_{T>0}$	$ER_{T=0}$	LPD	$LD_{T>0}$	$LD_{T=0}$	CD	CCD	NC
λ	13	13	3	15	15	7	7	7
ν	32	23	12	32	23	12	10	16
χ	64	64	4	64	64	8	8	8
$\tilde{J}$	36	25	16	36	25	16	16	20

herence models. For comparison, in the elementary operator basis $\{|i_1 i_2\rangle\langle j_1 j_2|\}$, we have $\lambda=\nu$ [see Eq. (28)], and then the significantly larger number of nonzero elements is given by the second row in Table I [the number of nonzero elements of ν equals that of $\boldsymbol{L}$]. Since Eq. (55) is only an approximation, the number of nonzero elements of the matrix χ is larger than that for λ; it is shown in the third row of Table I for the Pauli basis. For the elementary basis [then $\chi=\tilde{J}$, see Eq. (21)] this number is shown in the fourth row and is typically significantly larger (except for the models with energy relaxation). This illustrates the convenience of the Pauli basis.

The nonlocality parameters ϵ_{NL} and ϵ'_{NL} introduced by Eqs. (34) and (38) approximately coincide in the weak-decoherence case (55); ϵ'_{NL} is time independent, while ϵ_{NL} slowly changes with time. Calculation of ϵ'_{NL} gives the following results for the considered decoherence models. For the local decoherence involving both energy relaxation and pure dephasing, we obtain $\epsilon'_{NL}=0$, as should be expected. For the model of correlated pure dephasing with $\Gamma_1=\Gamma_2$, the nonlocality parameter $\epsilon'_{NL}=2|\kappa|/(1+\sqrt{1+\kappa^2})$ depends on the correlation factor κ, so that $\epsilon'_{NL}\approx|\kappa|$ for $|\kappa|\ll 1$ and $\epsilon'_{NL}=2\sqrt{2}-2\approx 0.83$ for $\kappa=\pm 1$. Finally, for a noisy coupling $\epsilon'_{NL}=2\sqrt{2}-1\approx 1.83$. As expected, ϵ'_{NL} is on the order of 1 for a strongly nonlocal decoherence.

D. Effects of decoherence on the $\sqrt{i\text{SWAP}}$ gate

Now let us consider the effects of decoherence on the χ matrix of the $\sqrt{i\text{SWAP}}$ gate. We calculate χ via Eq. (21) from the evolution equation $\mathcal{L}=e^{(\boldsymbol{L}_{coh}+\boldsymbol{L})\pi/2S}$, where $\boldsymbol{L}_{coh}$ is given by Eqs. (25) and (39), and 16×16 matrix $\boldsymbol{L}$ depends on the decoherence model (Sec. V B).

In the important case of weak decoherence the first-order approximation (29) leads to the linear relation between the decoherence contribution $\chi-\chi_{ideal}$ and the decoherence generator $\boldsymbol{L}$ (the evolution time is fixed). Therefore, since the decoherence generators for various mechanisms simply add up [see Eq. (54)], their contributions into the χ matrix are approximately additive for a weak decoherence,

$$\chi \approx \chi_{ideal} + \delta\chi_{loc} + \delta\chi_{CD} + \delta\chi_{NC}, \tag{59}$$

and we can consider them separately.

Figures 2–4 discussed below show the numerical results for the χ matrix of the $\sqrt{i\text{SWAP}}$ gate in the presence of the decoherence mechanisms considered in Sec. V B. A comparison of Fig. 1 with Figs. 2–4 shows that the effect of decoherence on the χ matrix is to modify the values of the nonzero elements of χ_{ideal} and generally to add extra nonzero elements. Below we identify patterns of extra elements specific for each considered decoherence mechanism, which allow for a fast, although tentative, identification of these mechanisms. For this purpose it is sufficient to consider only

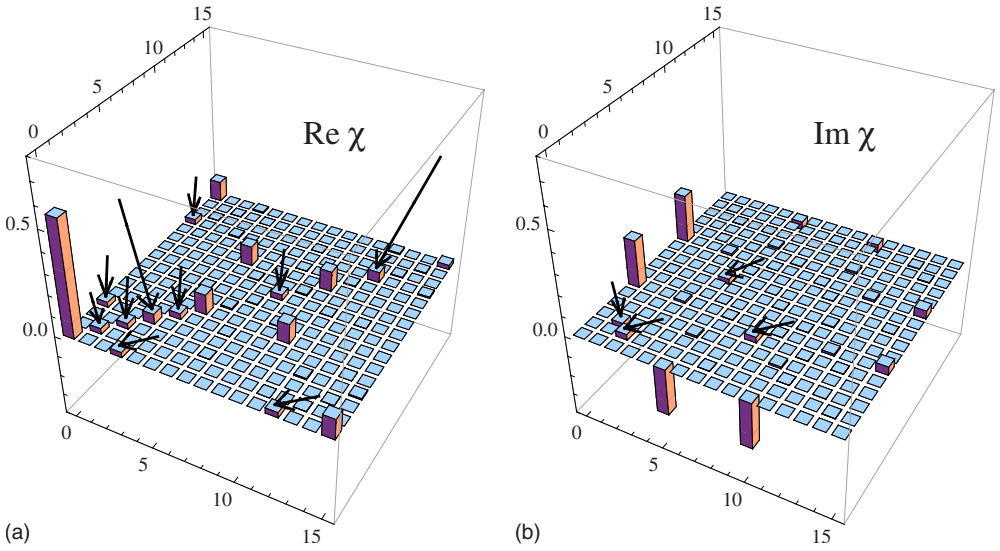

FIG. 2. (Color online) The process matrix χ (in the Pauli basis) for the $\sqrt{i\text{SWAP}}$ gate in the presence of local decoherence for $S/2\pi=20$ MHz, $T_1=90$ ns, and $T_2=60$ ns. The matrix elements marked by the long arrows, $\chi_{33}=\chi_{12,12}$, are the features of the pure dephasing, while the elements marked by the short arrows ($\chi_{11}=\chi_{22}=\chi_{44}=\chi_{88}$ and $\chi_{03}=\chi_{30}=\chi_{0,12}=\chi_{12,0}$ in Re χ and $\chi_{21}=-\chi_{12}=\chi_{84}=-\chi_{48}$ in Im χ) are the features of the energy relaxation.

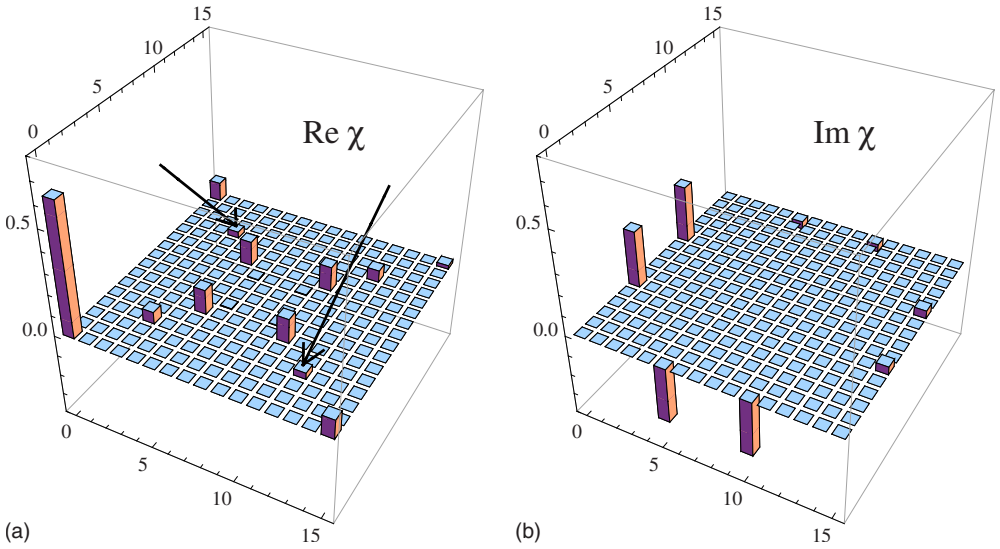

FIG. 3. (Color online) The χ matrix (in the Pauli basis) for the $\sqrt{i\mathrm{SWAP}}$ gate in the presence of correlated pure dephasing for $S/2\pi=20$ MHz, $\Gamma_{\mathrm{PD}}=(90\ \mathrm{ns})^{-1}$, and $\kappa=0.5$. Significant matrix elements shown by the arrows, $\chi_{3,12}=\chi_{12,3}$, indicate significant correlation of the two-qubit dephasing, $|\kappa|\sim 1$.

the largest extra elements (most significant out of the first-order in decoherence elements). An important observation (see below) is that for the considered decoherence models the positions of the largest extra elements of χ coincide with the positions of elements of λ discussed in the previous subsection. This makes the analysis of the χ matrix for the $\sqrt{i\mathrm{SWAP}}$ gate rather similar to the analysis in the absence of unitary evolution (Sec. V C), except for the noisy-coupling model for which there are no extra elements in χ. Consider now the effects of decoherence models in more detail.

1. Local decoherence

We focus on parameter values typical for experiments with the superconducting phase qubits, and therefore assume zero-temperature case (which is a very good approximation for the experiments [23–25,32–34]). We also assume the same local decoherence parameters for both qubits, so that $\Gamma_d^{(1)}=\Gamma_d^{(2)}=1/T_1$, $T_2^{(1)}=T_2^{(2)}=T_2$, and $\Gamma_u^{(1)}=\Gamma_u^{(2)}=0$.

Figure 2 shows the process matrix of the $\sqrt{i\mathrm{SWAP}}$ gate in the presence of local decoherence. For this example we have chosen the coupling $S/2\pi=20$ MHz (which is in between the coupling values of experiments [33,34]) and the decoherence parameters $T_1=90$ ns and $T_2=60$ ns, which are also more or less typical for the superconducting phase qubits (much longer relaxation times have been achieved recently [59,60]).

The local decoherence includes two mechanisms: energy relaxation (with the rate $1/T_1$) and pure dephasing (with the

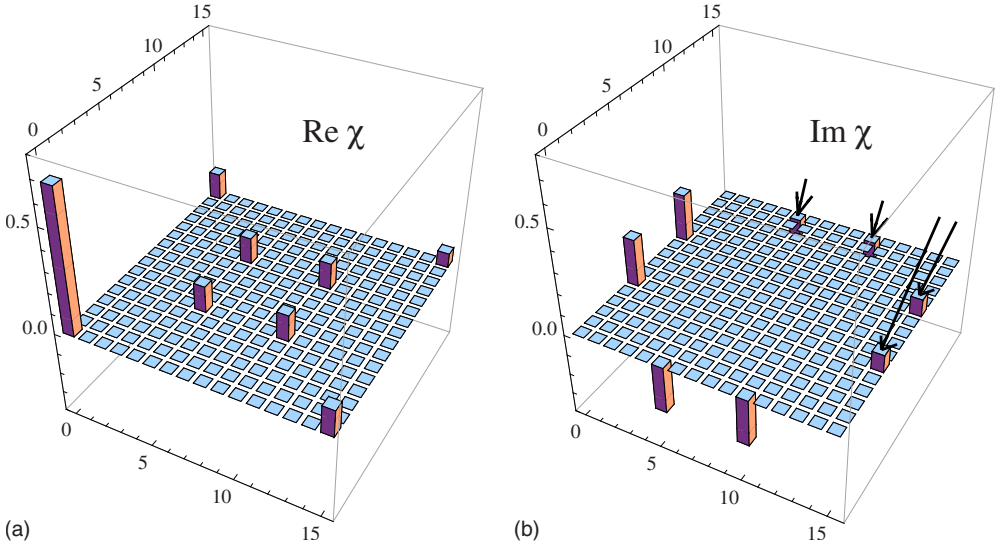

FIG. 4. (Color online) The χ matrix (in the Pauli basis) for the $\sqrt{i\mathrm{SWAP}}$ gate in the presence of a noisy coupling for $S/2\pi=20$ MHz and $\Gamma_s=(90\ \mathrm{ns})^{-1}$. The specific feature of the noisy coupling is the increase in the elements shown by the arrows in comparison with their ideal value $(\sqrt{2}-1)/8$.

rate $\Gamma_{\rm PD}=1/T_2-1/2T_1$). As follows from the results presented below, the relative strength of these two mechanisms can be easily estimated by inspection of the extra elements of χ (compared to $\chi_{\rm ideal}$) in Fig. 2. The elements marked by the long arrows are due to pure dephasing, while the elements marked by the short arrows are due to the energy relaxation. By comparing the height of the elements of χ marked by the long and the short arrows, one can crudely estimate the relative strength of these two mechanisms.

The largest extra elements for the energy-relaxation model (short arrows in Fig. 2) in the first order in $1/T_1$ are the following:

$$\chi_{11}=\chi_{22}=\chi_{44}=\chi_{88}=\frac{\pi+2\sqrt{2}}{16ST_1}\approx\frac{0.37}{ST_1},$$

$$\chi_{03}=\chi_{0,12}=\chi_{30}=\chi_{12,0}=\frac{\pi(2+\sqrt{2})}{32ST_1}\approx\frac{0.34}{ST_1},$$

$$\chi_{21}=\chi_{84}=-\chi_{12}=-\chi_{48}=i\frac{\pi+2\sqrt{2}}{16ST_1}\approx i\frac{0.37}{ST_1}. \quad (60)$$

They are at the same positions as the elements of λ [Eq. (56)] (the remaining element λ_{00} is at the location of the main $\sqrt{i\rm SWAP}$ peak, while we consider only extra elements of χ matrix).

We emphasize that the χ matrix also contains many other first order in $1/T_1$ elements (in contrast to the unity-gate case considered in the previous subsection); however, they happen to have relatively small absolute values. The largest of them are imaginary: $\chi_{46}=\chi_{4,11}=\chi_{13,6}=\chi_{13,11}=i\pi/(16\sqrt{2}ST_1)\approx 0.14i/ST_1$; this gives eight elements together with the corresponding Hermitian conjugated elements. There are also four elements of magnitude $0.06/ST_1$ and eight elements with the absolute value $0.02/ST_1$.

The rest of the extra elements of χ are of a higher order in $1/ST_1$, and therefore much smaller than the first-order elements for $ST_1\gg 1$. For instance, $\chi_{33}=\chi_{12,12}=\chi_{3,12}=\chi_{12,3}\approx(\pi^2/64)(ST_1)^{-2}$ (we show these elements explicitly because they are located at the same positions as the most significant elements for the model of pure dephasing discussed below).

For the model of local pure dephasing the largest (not all) first order in $\Gamma_{\rm PD}$ elements are

$$\chi_{33}=\chi_{12,12}\approx\frac{(3\pi+2)\Gamma_{\rm PD}}{16S}\approx\frac{0.71\Gamma_{\rm PD}}{S}, \quad (61)$$

and they are again at the same positions as the elements of λ in Eq. (57). These elements are shown by the long arrows in Fig. 2. Since for Fig. 2 we assumed $\Gamma_{\rm PD}=1/T_1$, the height of these elements is comparable to (approximately twice larger than) the height of the main extra elements due to the energy relaxation. The other (much smaller) first order in $\Gamma_{\rm PD}$ elements are discussed below, combined with the more general case of correlated pure dephasing, which we consider next.

2. Correlated dephasing

Let us consider the effects of correlated pure dephasing for $\Gamma_1=\Gamma_2\equiv\Gamma_{\rm PD}$ and arbitrary correlation factor $\kappa=\bar{\Gamma}/2\Gamma_{\rm PD}$. Now, χ generally contains eight extra elements, all of them real. These eight elements are also present in the first order in $\Gamma_{\rm PD}/S$; however, only four of them are relatively large:

$$\chi_{33}=\chi_{12,12}\approx\frac{[3\pi+2+(\pi-2)\kappa]\Gamma_{\rm PD}}{16S}$$

$$\approx(0.71+0.07\kappa)\Gamma_{\rm PD}/S, \quad (62a)$$

$$\chi_{3,12}=\chi_{12,3}\approx\frac{[\pi-2+(3\pi+2)\kappa]\Gamma_{\rm PD}}{16S}$$

$$\approx(0.07+0.71\kappa)\Gamma_{\rm PD}/S, \quad (62b)$$

while the other four elements are much smaller, $\chi_{66}=\chi_{99}=-\chi_{69}=-\chi_{96}\approx(\pi-2)(1-\kappa)\Gamma_{\rm PD}/(16S)\approx 0.07(1-\kappa)\Gamma_{\rm PD}/S$. Notice that the larger elements (62) are again at the positions of the elements of λ in Eq. (57), and these positions are all different from those for the energy relaxation. For a weak correlation, $\kappa\ll 1$, the elements $\chi_{3,12}$ and $\chi_{12,3}$ [see Eq. (62b)] become small, recovering result (61) for the local dephasing.

Figure 3 shows the χ matrix of the $\sqrt{i\rm SWAP}$ gate affected by the partially correlated dephasing, $\kappa=0.5$. The two diagonal extra elements, χ_{33} and $\chi_{12,12}$, are at the positions shown by the long arrows in Fig. 2, and their values are almost independent of κ. In contrast, the off-diagonal elements $\chi_{3,12}$ and $\chi_{12,3}$, marked by the arrows in Fig. 3, strongly depend on the correlation κ, so that their magnitudes are comparable to the values of χ_{33} and $\chi_{12,12}$ only for a significant correlation, $|\kappa|\sim 1$ [see Eq. (62b)]. This clearly suggests the way to check decoherence due to fluctuating common magnetic field in an experiment with phase qubits.

The χ matrix has especially simple form in the case of the completely correlated dephasing, $\kappa=1$, so that $\Gamma_-=0$, and $\Gamma_+=4\Gamma_{\rm PD}$ in Eq. (51). Then, the exact solution gives the following nonzero elements of χ. The elements which are at the positions of the nonzero elements of $\chi_{\rm ideal}$ become

$$\chi_{mn}=\frac{1}{8}\begin{pmatrix} f_+ & ig_+ & ig_+ & \gamma_d^4 \\ -ig_+ & 1 & 1 & -ig_- \\ -ig_+ & 1 & 1 & -ig_- \\ \gamma_d^4 & ig_- & ig_- & f_- \end{pmatrix}, \quad (63)$$

where $m,n=0,5,10,15$, $f_\pm=2+\gamma_d^4\pm 2\sqrt{2}\gamma_d$, $g_\pm=\sqrt{2}\gamma_d\pm 1$, and $\gamma_d=e^{-\pi\Gamma_{\rm PD}/2S}$. The extra nonzero matrix elements are

$$\chi_{33}=\chi_{3,12}=\chi_{12,3}=\chi_{12,12}=(1-e^{-2\pi\Gamma_{\rm PD}/S})/8, \quad (64)$$

so that all of them are equal [as for the first-order result (62) with $\kappa=1$]. Notice that for a partially correlated dephasing with $0<\kappa<1$ the exact solution gives $\chi_{33}=\chi_{12,12}>\chi_{3,12}=\chi_{12,3}>0$ (as in Fig. 3).

3. Noisy coupling

In contrast to the previous models, the matrix λ for the noisy-coupling decoherence [Eq. (58)] has nonzero elements

only at the positions, for which the matrix χ_{ideal} is also nonzero. As a result (not quite trivial), the noisy coupling does not produce extra elements in the χ matrix [neither in the first-order approximation (29) nor in the exact solution]. The exact solution gives the following nonzero elements of χ:

$$\chi_{mn} = \frac{1}{8}\begin{pmatrix} 3+2\sqrt{2}\gamma_c & ih_+ & ih_+ & 1 \\ -ih_+ & 1 & 1 & -ih_- \\ -ih_+ & 1 & 1 & -ih_- \\ 1 & ih_- & ih_- & 3-2\sqrt{2}\gamma_c \end{pmatrix}, \quad (65)$$

where $m,n=0,5,10,15$, $h_\pm=\sqrt{2}\gamma_c \pm \gamma_c^4$, and $\gamma_c=e^{-\pi\Gamma_s/2S}$. The χ matrix for $S/2\pi=20$ MHz and $\Gamma_s=1/(90\ \text{ns})$ is shown in Fig. 4.

Despite the noisy coupling does not produce extra elements in the χ matrix, this model also has its unique feature. Let us consider the imaginary elements $\chi_{5,15}$, $\chi_{10,15}$, $\chi_{15,5}$, and $\chi_{15,10}$ shown by the arrows in Fig. 4, which all have the same absolute value $h_-/8$. From the above formula it is easy to see that this value is larger than the ideal value $(\sqrt{2}-1)/8\approx 0.052$ (unless decoherence is very strong, $\Gamma_s/S>0.77$), with the maximum of 0.094 at $\Gamma_s/S=0.22$. In all other considered models the absolute value of these matrix elements decreases in comparison with the ideal case [see Figs. 1–3 and Eq. (63)], so their increase is a unique feature of the noisy coupling.

Notice that the absence of this evidence does not exclude the possibility of noisy coupling since the increase in the elements marked by the arrows in Fig. 4 may be compensated by the their decrease due to other decoherence mechanisms. Generally, the fast identification of decoherence models by their unique features should serve only as a preliminary step, while the accurate quantification of the decoherence mechanisms requires a numerical best-fit procedure.

E. Discussion

As observed and discussed above, for the considered decoherence models the positions of the largest extra elements in the χ matrix of the $\sqrt{i\text{SWAP}}$ gate coincide with the positions of nonzero elements of λ. Moreover, a comparison of Eqs. (60) and (62) with Eqs. (56) and (57) shows that for the largest extra elements $\chi_{mn}\approx\lambda_{mn}\tau_g$, where $\tau_g=\pi/2S$ is the gate-operation time [this statement is not correct for Eq. (62b) in the case $|\kappa|\ll 1$, but then the elements are small anyway]. This fact is not trivial and deserves a discussion.

Let us consider an arbitrary two-qubit entangling gate described by a Hamiltonian H with a characteristic frequency S. In the presence of a weak Markovian decoherence $\boldsymbol{L}$ the first-order approximation (29) gives the evolution map

$$\mathcal{L}(\tau_g) = e^{\boldsymbol{L}_{\text{coh}}\tau_g} + \int_0^{\tau_g} e^{\boldsymbol{L}_{\text{coh}}(\tau_g-\tau)}\boldsymbol{L}e^{\boldsymbol{L}_{\text{coh}}\tau}d\tau, \quad (66)$$

where τ_g is the gate-operation time. This matrix can be transformed into χ, giving the corresponding separation of terms $\chi=\chi_{\text{ideal}}+\delta\chi$. For a very short time, so that $S\tau_g\ll 1$, the exponential factors in Eq. (66) are close to 1, and therefore

$$\delta\chi \approx \lambda\tau_g, \quad (67)$$

seemingly explaining the fact observed above. The problem, however, is that a strongly entangling gate (such as $\sqrt{i\text{SWAP}}$) necessarily operates in the different regime, $S\tau_g\gtrsim 1$, for which the approximation (67) is not valid.

We have numerically checked the relative error of approximation (67) for the $\sqrt{i\text{SWAP}}$ gate by calculating the dimensionless parameter $\epsilon=\text{Tr}|\delta\chi-\lambda\tau_g|/\text{Tr}|\delta\chi|$, introduced similar to Eq. (34). As expected, we have obtained $\epsilon\sim 1$ (e.g., $\epsilon=0.54$ for the energy relaxation), confirming that approximation (67) is invalid. However, the inaccuracy ϵ happens to be mainly due to a large number of small nonzero elements in $\delta\chi$, while for the largest extra elements (where χ_{ideal} is zero) approximation (67) unexpectedly survives. The origin of this fact is still a puzzle for us. Nevertheless, the same useful property may hopefully be also valid for some other quantum gates and decoherence models.

F. Strongly detuned qubits

In Sec. V C we have calculated the χ matrix for the identity gate, which is realized when the two qubits are uncoupled. However, in many experimental realizations (e.g., for capacitively coupled phase qubits [33,34]) the qubits are permanently coupled, and effective uncoupling is produced by strong detuning of the qubits: $|\Delta\omega|\gg|S|$, where $\Delta\omega=\omega_{qb,1}-\omega_{qb,2}$ is the detuning. In such experiment it is natural to extract decoherence parameters from the χ matrices in both situations: resonant qubits ($\sqrt{i\text{SWAP}}$) and strongly detuned qubits (that gives a more straightforward access to decoherence parameters). In this subsection we analyze the χ matrix in the case of strongly detuned qubits.

To deal with detuned qubits we need to introduce a rotating frame, which rotates with different frequencies for different qubits. For this frame it is preferable to use the actual eigenfrequencies (shifted due to the level repulsion), even though we still use the basis of uncoupled states ($|01\rangle$, $|10\rangle$, etc.). This produces the Hamiltonian [which replaces Eq. (39)]

$$H = (\hbar/2)(\Delta\omega-\Delta\tilde{\omega})(|1\rangle\langle 1|\otimes I - I\otimes|1\rangle\langle 1|) + (\hbar S/2)(e^{-i\Delta\tilde{\omega}t}|01\rangle\langle 10| + e^{i\Delta\tilde{\omega}t}|10\rangle\langle 01|), \quad (68)$$

where $\Delta\tilde{\omega}=\sqrt{(\Delta\omega)^2+S^2}\,\text{sgn}(\Delta\omega)$ is the difference of eigenfrequencies (we define it with the same sign as for $\Delta\omega$), and the first term is due to the level repulsion. We assume a strong detuning, which means $|\Delta\tilde{\omega}|\approx|\Delta\omega|\gg|S|$; then the first term in Eq. (68) is small since $\Delta\tilde{\omega}-\Delta\omega\approx S^2/2\Delta\omega$.

For strongly detuned qubits, Eq. (55) for the identity gate χ matrix is somewhat modified, and at sufficiently small time t the χ matrix can be approximated as

$$\chi \approx \chi^I + \delta\chi^c + \lambda t, \quad (69)$$

where χ^I is for the ideal identity gate, the small correction $\delta\chi^c$ comes from the Hamiltonian (68), and the decoherence λ matrix is also somewhat modified (as discussed below).

The correction $\delta\chi^c$ oscillates in time with frequency $\Delta\tilde{\omega}$. After averaging over these fast oscillations, we get (in the first order in S) four nonzero terms

$$\delta\chi^c_{09} = \delta\chi^c_{60} = -\delta\chi^c_{06} = -\delta\chi^c_{90} = iS/4\Delta\tilde{\omega}. \quad (70)$$

If we do not average over time, then these terms should be multiplied by $(1-\cos\Delta\tilde{\omega}t)$; also there will be four more terms with zero average: $\delta\chi^c_{05}=\delta\chi^c_{0,10}=-\delta\chi^c_{50}=-\delta\chi^c_{10,0}=iS\sin(\Delta\tilde{\omega}t)/4\Delta\tilde{\omega}$. Notice that $\delta\chi^c$ is small only in the rotating frame based on the eigenfrequencies. If, for example, the rotating frame uses the unperturbed qubit frequencies, then both qubits will be slowly rotating about the z axis of the Bloch sphere that will eventually produce large terms $\delta\chi^c_{03}$, $\delta\chi^c_{30}$, $\delta\chi^c_{0,12}$, $\delta\chi^c_{12,0}$, $\delta\chi^c_{12,3}$, and $\delta\chi^c_{3,12}$. In an experiment the choice of the rotating frame corresponds to the choice of the reference microwave frequencies.

Now let us discuss contributions of the dephasing processes to the matrix λ. It can be shown that the contribution from the energy relaxation in qubits is still given by Eq. (56) (as for the identity gate); however, the up and down rates $\Gamma^{(\alpha)}_u$ and $\Gamma^{(\alpha)}_d$ for the two qubits ($\alpha=1,2$) can now be different from these rates for the qubits in resonance. The difference is because these rates are proportional to the Fourier components of the bath spectral density at the qubit frequencies $\pm\omega_{qb,\alpha}$, and therefore changing qubit frequencies may noticeably change the rates. For pure dephasing the contribution to the λ matrix is still given by Eq. (57) (as for the identity gate) without any changes.

In contrast, the contribution to the λ matrix due to the noisy coupling $S+s(t)$ significantly differs from Eq. (58) for the identity gate. This comes from a significant change in Eq. (53) when we take into account the modified Hamiltonian (68). First, the rate $\Gamma_s=(1/4)\int_0^\infty\langle s(0)s(t)\rangle dt$ should now be replaced with $\Gamma'_s=(1/4)\int_0^\infty\langle s(0)s(t)\rangle\cos(\Delta\tilde{\omega}t)dt$. This would lead to a negligible change if the correlation time $\tau_c^{\rm NC}$ of the noise $s(t)$ is short: $\tau_c^{\rm NC}\ll 1/|\Delta\tilde{\omega}|$; however $\Gamma'_s\ll\Gamma_s$ for a long correlation time: $\tau_c^{\rm NC}\gg 1/|\Delta\tilde{\omega}|$. The second change in Eq. (53) is that we should delete the term ρ_{21} in the second row and similarly the term ρ_{12} in the third row (this simple change happens in the secular approximation, $\Gamma'_s\ll|\Delta\tilde{\omega}|$). As a result of the changes, the contribution to the λ matrix due to noisy coupling has now the following nonzero elements:

$$\lambda_{00}=-\Gamma'_s,\quad \lambda_{0,15}=\lambda_{15,0}=\Gamma'_s/2,$$

$$\lambda_{55}=\lambda_{10,10}=\lambda_{5,10}=\lambda_{10,5}=\lambda_{66}=\lambda_{99}=\Gamma'_s/4,$$

$$\lambda_{69}=\lambda_{96}=-\Gamma'_s/4. \quad (71)$$

Notice four additional positions of nonzero elements in this matrix compared to the identity gate case (58).

It is important to mention that positions of nonzero elements of $\delta\chi^c$ and nonzero elements of λ for various decoherence models are still all different (except element λ_{00}, which is nonzero even in χ^I, and elements $\lambda_{0,15},\lambda_{15,0}$ which appear in both correlated dephasing and noisy coupling). Therefore, measuring χ matrix experimentally for strongly detuned qubits gives an easy way to find main decoherence mechanisms and quantify their parameters. Notice that measuring χ matrix (69) for several times t gives a more accurate value for λ by a simple least-squares method and also allows for checking the linearity in time, which essentially checks that decoherence is Markovian.

VI. CONCLUSION

In this paper we have discussed the effects of decoherence on the quantum process tomography of a quantum gate. In particular, we have introduced (Sec. IV) dimensionless parameters obtainable from experimental QPT results, which characterize nonlocality of decoherence. As an important practical example (Sec. V), we have analyzed the process matrix χ for the two-qubit $\sqrt{i\rm SWAP}$ gate in the presence of several local and nonlocal decoherence mechanisms, typical for superconducting phase qubits. Besides presenting explicit results for the χ matrix in the presence of decoherence (using the Pauli basis), we have focused on finding specific patterns for each decoherence model. These patterns may be used for a fast identification of the most important decoherence mechanisms in an experiment, that is an alternative to the laborious procedure of numerical best fitting of experimental χ matrix. Somewhat unexpectedly, we have found that these patterns for the considered decoherence models are to a large extent the same for the $\sqrt{i\rm SWAP}$ and identity gates. In future it is interesting to study whether or not our fast-identification approach can be applied to other quantum gates and decoherence mechanisms.

ACKNOWLEDGMENTS

The work was supported by NSA and DTO under ARO Grant No. W911NF-08-1-0336.

APPENDIX: SOME PROPERTIES OF THE PROCESS MATRIX χ

(1) Let us consider the change in the matrix χ under a linear transformation of the basis $\{E_n\}\to\{E'_n\}$. From Eq. (6), using the substitution $E_n=\sum_{n,n'=0}^{d^2-1}V_{n'n}E'_{n'}$, where V is the $d^2\times d^2$ transformation matrix (while E_n are $d\times d$ matrices), we obtain $\rho=\sum_{m,n=0}^{d^2-1}\chi'_{mn}E'_m\rho^0E'^\dagger_n$ with

$$\chi'=V\chi V^\dagger. \quad (A1)$$

If the both bases are orthogonal, so that $\mathrm{Tr}(E_n^\dagger E_m)=Q\delta_{nm}$ and $\mathrm{Tr}(E'^\dagger_n E'_m)=Q'\delta_{nm}$, then $V_{nm}=\mathrm{Tr}(E'^\dagger_n E_m)/Q'$; in this case, $\sqrt{Q'/Q}V$ is a unitary matrix.

(2) Let us consider the transformation of the χ matrix under unitary transformations of the initial and final states, $\rho\to\rho'=U\rho U^\dagger$ and $\rho^0\to\rho'_0=U_0\rho^0U_0^\dagger$, where U and U_0 are unitary operators. From Eq. (6) we obtain $\rho'=\sum_{m,n=0}^{d^2-1}\chi_{mn}E'_m\rho'_0E'^\dagger_n$, where $E'_n=UE_nU_0^\dagger$, so the extra evolution of states corresponds to the transformation of the basis E_n. If the operators E_n are orthogonal, $\mathrm{Tr}(E_n^\dagger E_m)=Q\delta_{nm}$, then also $\mathrm{Tr}(E'^\dagger_n E'_m)=Q\delta_{nm}$ and, as follows from the previous paragraph,

$$\rho'=\sum_{m,n=0}^{d^2-1}\chi'_{mn}E_m\rho'_0E_n^\dagger, \quad (A2)$$

with χ' given by Eq. (A1), in which V is now a unitary matrix with the elements $V_{nm}=\mathrm{Tr}(E_n^\dagger E'_m)/Q=\mathrm{Tr}(E_n^\dagger UE_mU_0^\dagger)/Q$.

(3) Let us obtain the χ matrix for an evolution $\rho=K\rho^0K^\dagger$ with an arbitrary linear operator K. The most important special case is the unitary evolution (then K is unitary); however, in general K is an arbitrary Kraus operator [1]. Representing K in the operator basis E_n as

$$K=\sum_{n=0}^{d^2-1} k_nE_n \tag{A3}$$

and comparing the evolution equation with Eq. (6), we obtain

$$\chi_{mn}=k_mk_n^*. \tag{A4}$$

Notice that for the orthogonal basis, $\mathrm{Tr}(E_n^\dagger E_m)=Q\delta_{nm}$, the coefficients in Eq. (42) can be calculated as

$$k_n=\mathrm{Tr}(E_n^\dagger K)/Q. \tag{A5}$$

(4) As a simple example, let us consider the process matrix χ^I for the identity map. In this case $J^I_{\langle ik\rangle\langle jl\rangle}=\mathcal{L}^I_{\langle ij\rangle\langle kl\rangle}=\delta_{ik}\delta_{jl}$, and from Eq. (13) we obtain

$$\chi^I_{mn}=\sum_{i,j=0}^{d-1}(\boldsymbol{E}^{-1})_{m\langle ii\rangle}(\boldsymbol{E}^{-1})^*_{n\langle jj\rangle}. \tag{A6}$$

For the orthogonal basis, $\mathrm{Tr}(E_n^\dagger E_m)=Q\delta_{nm}$, from Eqs. (A4) and (A5) with $K=I$, we find

$$\chi^I_{mn}=Q^{-2}(\mathrm{Tr}\,E_m)^*\mathrm{Tr}\,E_n. \tag{A7}$$

This equation further simplifies when $\mathrm{Tr}\,E_n=0$ for all n except for, say, $n=0$ (as in the case of the Pauli basis). Then the basis orthogonality yields $E_0=\sqrt{Q/d}I$, and Eq. (A7) becomes

$$\chi^I_{mn}=(d/Q)\delta_{m0}\delta_{n0}. \tag{A8}$$

For the usual normalization $Q=d$, it becomes $\chi^I_{mn}=\delta_{m0}\delta_{n0}$.

[1] M. A. Nielsen and I. L. Chuang, *Quantum Computation and Quantum Information* (Cambridge University Press, Cambridge, England, 2000).
[2] J. F. Poyatos, J. I. Cirac, and P. Zoller, Phys. Rev. Lett. **78**, 390 (1997).
[3] I. L. Chuang and M. A. Nielsen, J. Mod. Opt. **44**, 2455 (1997).
[4] D. W. Leung, Ph.D. thesis, Stanford University, 2000; J. Math. Phys. **44**, 528 (2003).
[5] G. M. D'Ariano and P. Lo Presti, Phys. Rev. Lett. **86**, 4195 (2001).
[6] G. M. D'Ariano and P. Lo Presti, Phys. Rev. Lett. **91**, 047902 (2003).
[7] J. B. Altepeter, D. Branning, E. Jeffrey, T. C. Wei, P. G. Kwiat, R. T. Thew, J. L. O'Brien, M. A. Nielsen, and A. G. White, Phys. Rev. Lett. **90**, 193601 (2003).
[8] M. Mohseni and D. A. Lidar, Phys. Rev. Lett. **97**, 170501 (2006).
[9] M. Mohseni, A. T. Rezakhani, and D. A. Lidar, Phys. Rev. A **77**, 032322 (2008).
[10] M. W. Mitchell, C. W. Ellenor, S. Schneider, and A. M. Steinberg, Phys. Rev. Lett. **91**, 120402 (2003).
[11] A. Mazzei, M. Ricci, F. De Martini, and G. M. D'Ariano, Fortschr. Phys. **51**, 342 (2003).
[12] J. L. O'Brien, G. J. Pryde, A. Gilchrist, D. F. V. James, N. K. Langford, T. C. Ralph, and A. G. White, Phys. Rev. Lett. **93**, 080502 (2004).
[13] Y. Nambu and K. Nakamura, Phys. Rev. Lett. **94**, 010404 (2005).
[14] N. K. Langford, T. J. Weinhold, R. Prevedel, K. J. Resch, A. Gilchrist, J. L. O'Brien, G. J. Pryde, and A. G. White, Phys. Rev. Lett. **95**, 210504 (2005).
[15] N. Kiesel, C. Schmid, U. Weber, R. Ursin, and H. Weinfurter, Phys. Rev. Lett. **95**, 210505 (2005).
[16] Z.-W. Wang, Y.-S. Zhang, Y.-F. Huang, X.-F. Ren, and G.-C. Guo, Phys. Rev. A **75**, 044304 (2007).
[17] A. M. Childs, I. L. Chuang, and D. W. Leung, Phys. Rev. A **64**, 012314 (2001).
[18] Y. S. Weinstein, T. F. Havel, J. Emerson, N. Boulant, M. Saraceno, S. Lloyd, and D. G. Cory, J. Chem. Phys. **121**, 6117 (2004).
[19] H. Kampermann and W. S. Veeman, J. Chem. Phys. **122**, 214108 (2005).
[20] M. Riebe, K. Kim, P. Schindler, T. Monz, P. O. Schmidt, T. K. Körber, W. Hänsel, H. Häffner, C. F. Roos, and R. Blatt, Phys. Rev. Lett. **97**, 220407 (2006).
[21] T. Monz, K. Kim, W. Hänsel, M. Riebe, A. S. Villar, P. Schindler, M. Chwalla, M. Hennrich, and R. Blatt, Phys. Rev. Lett. **102**, 040501 (2009).
[22] M. Howard, J. Twamley, C. Wittmann, T. Gaebel, F. Jelezko, and R. Wrachtrup, New J. Phys. **8**, 33 (2006).
[23] M. Neeley, M. Ansmann, R. C. Bialczak, M. Hofheinz, N. Katz, E. Lucero, A. O'Connell, H. Wang, A. N. Cleland, and J. M. Martinis, Nat. Phys. **4**, 523 (2008).
[24] N. Katz, M. Neeley, M. Ansmann, R. C. Bialczak, M. Hofheinz, E. Lucero, A. O'Connell, H. Wang, A. N. Cleland, J. M. Martinis, and A. N. Korotkov, Phys. Rev. Lett. **101**, 200401 (2008).
[25] R. C. Bialczak, M. Ansmann, N. Katz, E. Lucero, R. McDermott, M. Neeley, A. D. O'Connell, M. Steffen, E. Weig, A. Cleland, and J. M. Martinis, Bull. Am. Phys. Soc. **52**, P33.00010 (2007); R. C. Bialczak, M. Ansmann, M. Hofheinz, E. Lucero, M. Neeley, A. O'Connell, D. Sank, M. Steffen, H. Wang, J. Wenner, A. Cleland, and J. M. Martinis, *ibid.* **54**, J17.00002 (2009).
[26] N. Boulant, T. F. Havel, M. A. Pravia, and D. G. Cory, Phys. Rev. A **67**, 042322 (2003).
[27] J. Emerson, M. Silva, O. Moussa, C. Ryan, M. Laforest, J. Baugh, D. G. Cory, and R. Laflamme, Science **317**, 1893 (2007).
[28] A. Bendersky, F. Pastawski, and J. P. Paz, Phys. Rev. Lett. **100**, 190403 (2008).
[29] M. M. Wolf, J. Eisert, T. S. Cubitt, and J. I. Cirac, Phys. Rev. Lett. **101**, 150402 (2008).
[30] M. Mohseni, A. T. Rezakhani, and A. Aspuru-Guzik, Phys.

Rev. A **77**, 042320 (2008).
[31] M. Mohseni and A. T. Rezakhani, Phys. Rev. A **80**, 010101(R) (2009).
[32] J. M. Martinis, S. Nam, J. Aumentado, and C. Urbina, Phys. Rev. Lett. **89**, 117901 (2002); Y. Yu, S. Han, X. Chu, S.-I. Chu, and Z. Wang, Science **296**, 889 (2002); A. J. Berkley, H. Xu, R. C. Ramos, M. A. Gubrud, F. W. Strauch, P. R. Johnson, J. R. Anderson, A. J. Dragt, C. J. Lobb, and F. C. Wellstood, *ibid.* **300**, 1548 (2003); J. Claudon, F. Balestro, F. W. J. Hekking, and O. Buisson, Phys. Rev. Lett. **93**, 187003 (2004).
[33] R. McDermott, R. W. Simmonds, M. Steffen, K. B. Cooper, K. Cicak, K. D. Osborn, S. Oh, D. P. Pappas, and J. M. Martinis, Science **307**, 1299 (2005).
[34] M. Steffen, M. Ansmann, R. C. Bialczak, N. Katz, E. Lucero, R. McDermott, M. Neeley, E. Weig, A. Cleland, and J. M. Martinis, Science **313**, 1423 (2006).
[35] E. B. Davis, *Quantum Theory of Open Systems* (Academic, London, 1976).
[36] A. Fujiwara and P. Algoet, Phys. Rev. A **59**, 3290 (1999).
[37] Y.-x. Liu, L. F. Wei, and F. Nori, EPL **67**, 874 (2004); Phys. Rev. B **72**, 014547 (2005).
[38] A. Gilchrist, N. K. Langford, and M. A. Nielsen, Phys. Rev. A **71**, 062310 (2005).
[39] M.-D. Choi, Linear Algebr. Appl. **10**, 285 (1975).
[40] A. Jamiolkowski, Rep. Math. Phys. **3**, 275 (1972).
[41] T. F. Havel, J. Math. Phys. **44**, 534 (2003).
[42] D. Salgado, J. L. Sanchez-Gomez, and M. Ferrero, Open Syst. Inf. Dyn. **12**, 55 (2005).
[43] A. G. Kofman (unpublished).
[44] C. Cohen-Tannoudji, J. Dupont-Roc, and G. Grynberg, *Atom-Photon Interactions* (Wiley, New York, 1992).
[45] A. G. Kofman, Q. Zhang, J. M. Martinis, and A. N. Korotkov, Phys. Rev. B **75**, 014524 (2007).
[46] M. J. Bremner, C. M. Dawson, J. L. Dodd, A. Gilchrist, A. W. Harrow, D. Mortimer, M. A. Nielsen, and T. J. Osborne, Phys. Rev. Lett. **89**, 247902 (2002).
[47] N. Schuch and J. Siewert, Phys. Rev. A **67**, 032301 (2003).
[48] A. Imamoglu, D. D. Awschalom, G. Burkard, D. P. DiVincenzo, D. Loss, M. Sherwin, and A. Small, Phys. Rev. Lett. **83**, 4204 (1999).
[49] P. Samuelsson, E. V. Sukhorukov, and M. Büttiker, Phys. Rev. Lett. **91**, 157002 (2003).
[50] C. W. J. Beenakker, C. Emary, M. Kindermann, and J. L. van Velsen, Phys. Rev. Lett. **91**, 147901 (2003).
[51] T. Yu and J. H. Eberly, Phys. Rev. Lett. **93**, 140404 (2004); **97**, 140403 (2006).
[52] D. Tolkunov, V. Privman, and P. K. Aravind, Phys. Rev. A **71**, 060308(R) (2005).
[53] A. G. Kofman and A. N. Korotkov, Phys. Rev. A **77**, 052329 (2008).
[54] A. G. Kofman, e-print arXiv:0804.4167.
[55] K. Rabenstein and D. V. Averin, Turk. J. Phys. **27**, 313 (2003).
[56] L. F. Wei, Y.-X. Liu, M. J. Storcz, and F. Nori, Phys. Rev. A **73**, 052307 (2006).
[57] A. G. Redfield, IBM J. Res. Dev. **1**, 19 (1957).
[58] K. Blum, *Density Matrix Theory and Applications* (Plenum, New York, 1981).
[59] M. Hofheinz, E. M. Weig, M. Ansmann, R. C. Bialczak, E. Lucero, M. Neeley, A. D. O'Connell, H. Wang, J. M. Martinis, and A. N. Cleland, Nature (London) **454**, 310 (2008).
[60] J. M. Martinis, Quantum Inf. Process. **8**, 81 (2009).